Self-consistent modelling of L and H confinement modes and H-mode pedestal characteristics

D. Kalupin, M.Z. Tokar, B. Unterberg

Institut für Plasmaphysik, Forschungszentrum Jülich GmbH, EURATOM Association, D-52425 Jülich, Germany

e-mail contact: d.kalupin@fz-juelich.de

Abstract. The results of self-consistent modelling by the one-dimensional transport code RITM of plasma parameters in Low (L) and High (H) confinement modes, with particular stress on the edge transport barrier in the H-mode, are presented and discussed. The transport model used under both L and H-mode conditions includes contributions from Ion Temperature Gradient (ITG), Dissipative Trapped Electrons (DTE), Drift Alfven (DA) and Drift Resistive Ballooning (DRB) instabilities described in fluid approximation. The model predicts formation of the edge transport barrier at a high enough heating power due to the reduction of contributions from ITG and DA modes, dominating the edge transport in the L-mode, caused by the density gradient and by the pressure gradient and low collisionality, respectively.

1. Introduction

By analysing the cause of transport reduction at the edge under H-mode conditions, one have to take into account the contributions from instabilities of different nature. There are specific edge instabilities, e.g., DA or DRB modes, which are maintained by coulomb collisions and, therefore, are more intensive at a low temperature. Numerical modelling of edge turbulence [1] predicts that the shear of $E \times B$ rotation alone is not sufficient to stabilise these instabilities and low plasma collisionality and high pressure gradient are required for this. The latter factors are taken into account in an analytical model for DA turbulence developed in Ref.[2]. This model predicts that DA contribution to transport coefficients, controlling the edge turbulence under L-mode conditions, reduces drastically if the heating power exceeds a critical value. A predictive modelling of H-mode based on this model for DA turbulent transport was first performed in Ref.[3].

The suppression of specific edge turbulence is necessary but not enough for formation of the H-mode pedestal. Additionally, the drift modes, which dominate transport in the plasma core, should be damped in the barrier region. Normally it is assumed that the shear of the radial electric field is responsible for this[4]. However, the core turbulence in the H-mode without internal transport barriers is dominated by toroidal ITG instability (see, e.g., [5]). This develops when the temperature gradient exceeds a critical level[6], essentially determined by the density gradient. The latter increases to the plasma edge due to ionisation of neutrals recycling through the separatrix into the confined volume. This provides an additional to the $\mathbf{E} \times \mathbf{B}$ rotation shear channel for ITG suppression at the edge. It is demonstrated in our calculations that only if the effect of the density gradient on ITG turbulence is taken into account, important experimentally observed features of L-H transition and scalings for edge barrier characteristics can be explained.

2. RITM-code, transport model

The numerical modelling of L- and H-mode plasmas in JET has been performed by the one-dimensional transport code RITM [7]. This code allows modelling of the confined plasma region from plasma axis to separatrix in order to provide the dependencies of diverse plasma parameters on the effective minor radius of the magnetic surfaces, r. For neutrals produced by plasma recycling on divertor plates and entering confined volume through separatrix, a kinetic equation for the velocity distribution function f_n:

$$\frac{1}{g_1}\frac{\partial}{\partial r}\left(v_r f_n\right) = S_n - \nu_n f_n \tag{1}$$

where v_r, S_n and ν_n are the radial velocity, source density and ionisation frequency of neutral particles, respectively, is solved in a diffusive approximation.
The transport of electrons and impurity ions is described by continuity equations:

$$\frac{\partial n_e}{\partial t} + \frac{1}{rg_1}\frac{\partial}{\partial r}\left(rg_2\Gamma_\perp^e\right) = S_n + \sum_Z ZS_Z \tag{2}$$

$$\frac{\partial n_Z}{\partial t} + \frac{1}{rg_1}\frac{\partial}{\partial r}\left(rg_2\Gamma_\perp^Z\right) = S_Z \tag{3}$$

where $n_{e,Z,}$ are the densities of the electrons and impurity species of the charge Z, and $S_{n,Z}$ are their source densities (all ionisation stages of He, C, O, Ne, Si and Ar can be taken into consideration).
The particle flux densities include both diffusive and convective contributions:

$$\Gamma_\perp^e = -D_\perp\frac{\partial n_e}{\partial r} + V_\perp n_e, \quad \Gamma_\perp^Z = -D_\perp^Z\frac{\partial n_Z}{\partial r} + V_\perp^Z n_Z \tag{4}$$

The densities and fluxes of the background ions are computed from the quasi-neutrality conditions:

$$n_i = n_e - \sum Z\cdot n_Z, \quad \Gamma_\perp^i = \Gamma_\perp^e - \sum Z\cdot\Gamma_\perp^Z \tag{5}$$

The metric coefficients $g_{1,2}$ are determined by using the Shafranov shift calculated from the Grad-Shafranov equation and analytically prescribed elongation and triangularity of the magnetic surfaces.
The electron and ion temperatures T_e and T_i are computed by solving heat transport equations:

$$\frac{3}{2}\frac{\partial n_e T_e}{\partial t} + \frac{1}{rg_1}\frac{\partial}{\partial r}\left[rg_2\left(1.5\Gamma_\perp^e T_e - \kappa_\perp^e\frac{\partial T_e}{\partial r}\right)\right] = \frac{J^2}{\sigma} + Q_{au}^e - Q_{ei} - Q_{en} - Q_{eI} \tag{6}$$

$$\frac{3}{2}\frac{\partial n_\Sigma T_i}{\partial t} + \frac{1}{rg_1}\frac{\partial}{\partial r}\left[rg_2\left(1.5\Gamma_\perp^\Sigma T_i - \kappa_\perp^\Sigma\frac{\partial T_i}{\partial r}\right)\right] = Q_{au}^i + Q_{ei} + Q_{in} \tag{7}$$

where $n_\Sigma = n_i + \Sigma n_Z$, $\Gamma_\Sigma = \Gamma_i + \Sigma\Gamma_Z$ are the total ion density and their flux, $Q_{au}^{e,i}$ the electron and ion heat source due to additional heating from NBI and ICRH, whose radial profiles are taken from TRANSP calculations, Q_{ei}, Q_{en}, Q_{eI} the energy losses from electrons due to coulomb collisions with ions, excitation and ionisation of neutrals and impurities, respectively, Q_{in} the energy exchange between main ions and neutrals.
The boundary conditions of Eqs.(2),(3),(6) and (7) at the separatrix, $r = a$, imply the e-folding lengths of parameters, which are taken from measurements.

Transport model.
The present transport model in RITM takes into account the most important unstable drift modes. The corresponding contributions to the transport coefficients are

determined in a mixing length approximation [6], $D \approx \dfrac{\gamma_{\max}}{k_{\perp,\max}^2}$. Here $\gamma_{\max}$ is the maximum value of the instability linear growth rate γ considered as a function of the perpendicular wave number $k_\perp$ and $k_{\perp,\max}$ is the $k_\perp$-value where $\gamma_{\max}$ is approached. This leads to the following expressions for the contributions from ITG and DTE modes [6,8]:

$$D^{ITG} = \frac{cT_e}{k_{\perp,\max}^{ITG} eB}\left[\left(-\frac{d\ln T_i}{dr} + \frac{2}{3}\frac{d\ln n_e}{dr}\right)\left(Z_{eff}R\right)^{-1} - \frac{1}{8}\left(\frac{d\ln n_e}{dr} + \frac{2}{R}\right)^2 - \frac{20}{9}\frac{1}{R^2 Z_{eff}^2}\right]^{1/2} \quad (8)$$

$$D^{DTE} = \rho_s f_{tr}\eta_e\omega_* \frac{\omega_*\nu_{eff}}{\omega_*^2 + \nu_{eff}^2} \quad (9)$$

where c is the speed of light, e the elementary charge, B the magnetic field induction, Z_{eff} the ion effective charge, R the plasma major radius, ρ_s the ion Larmor radius, f_{tr} the fraction of trapped particles, $\omega_* = \dfrac{cT_e k_{\perp,\max}^{DTE}}{eB}\left(-\dfrac{d\ln n_e}{dr}\right)$ the electron drift frequency, $\nu_{eff} = \nu_{ei}R/r$ the effective collision frequency of trapped electrons with ν_{ei} being the collision frequency of thermal electrons, $k_{\perp,\max}^{ITG} = 0.3/\rho_s$ and $k_{\perp,\max}^{DTE} = 1/\rho_s$. The generalisation of D^{ITG} on the case of impure plasmas with $Z_{eff} > 1$ was performed by taking into account the results of modelling of ITG instability in multi-species plasmas [9].

The transport due to ITG and DTE modes is significantly reduced at the plasma edge due to strong density gradient and decreasing temperature, respectively. Here DA and DRB instabilities dominate the transport. The corresponding contributions are computed according to the formulas from Refs. [2] and [10], respectively:

$$D^{DA} = \frac{\chi_{GB}}{\sqrt{\mu}}\bar{\bar{\chi}}_\perp(\beta_n, \nu_n) \quad (10)$$

$$D^{DRB} \propto (2q\rho_e)^2 \nu_e R\left(-\frac{d\ln n_e}{dr}\right). \quad (11)$$

Here $\chi_{GB} = \rho_s^2 c_s / L_p$ is the Gyro-Bohm diffusion with c_s being the ion sound velocity and $L_p = -1/(d\ln P/dr)$ the pressure e-folding length; $\mu = -k_\parallel V_{The} L_p / c_s$ with $k_\parallel \sim 1/qR$ and V_{the} thermal electron velocity; the dimensionless factor $\bar{\bar{\chi}}_\perp(\beta_n,\nu_n) = \left[\dfrac{\left(1+\beta_n^2\right)^{-3} + \nu_n^2}{1+\beta_n^2+\nu_n^{4/3}}\right]^{1/2}$ depends on parameters $\beta_n = \left(\dfrac{M_i}{m_e}\right)^{1/2}\dfrac{4\pi n_e T_e}{B^2}\dfrac{1}{k_\parallel L_p}$ and $\nu_n = \left(\dfrac{M_i}{m_e}\right)^{1/4}\dfrac{L_p^{1/2}}{\lambda_e k_\parallel^{1/2}}$, being the normalised plasma beta and electron collision frequency, respectively, λ_e the mean three path length, q the safety factor and ρ_e the electron Larmor radius.

The drift-Alfven contribution starts to decrease with increasing pressure gradient formula when β_n exceeds a critical value of $1+\nu_n^{2/3}$. In Ref. [2] this condition has been used for an estimate of a critical edge temperature for a L-H transition.

Finally, the transport coefficients are assumed in the form:

$$D_\perp^e = D^{ITG} f_{tr} + D^{DTE} + D^{DRB} + D^{DA}, \tag{12}$$

$$V_\perp^e = \left[D^{ITG} f_{tr}(4r/3R) + D^{DTE}\right](d\ln q/dr), \tag{13}$$

$$D_\perp^Z = D_\perp, \tag{14}$$

$$V_\perp^Z = V_\perp^e + V_\perp^{Z,NEO} \tag{15}$$

$$\kappa_\perp^e = 3/2\left(D^{ITG} f_{tr} + D^{DTE} + D^{DRB} + D^{DA}\right)n_e, \tag{16}$$

$$\kappa_\perp^i = \kappa_\perp^{i,NEO} + 3/2\left(D^{ITG} + D^{DRB} + D^{DA}\right) \tag{17}$$

In the linear electrostatic approximation ITG instability does not provide particle transport. However, as other drift instabilities on the non-linear turbulent stage, ITG leads to stochastization of closed drift orbits and to particle losses. At easiest this happens to trapped electrons with low parallel velocity [11]. This explains the proportionality of the corresponding contribution to $D_\perp^e$ to the fraction of trapped particles, f_{tr}. In the expression for the electron pinch-velocity the small factor $4r/3R$ represents a relatively weak effect of ion driven modes on electron convection [12]. The impurity ion diffusion is assumed the same as for electrons; their pinch velocity, Eq.(15), is compound from anomalous and neo-classical contributions determined by the gradients of the density and temperature of background ions [13].

Up to now the non-linear dependence of transport coefficients on the plasma parameters and their radial gradients does not permit the convergence of RITM calculations for time steps smaller than ~ 10 ms. Therefore the ELM activity can not be presently modelled by RITM explicitly and the ELM effect on the transport is taken into account as its exponential increase when the pressure gradient exceeds the limit for MHD ballooning modes.

3. Modelling of L- and H-mode conditions

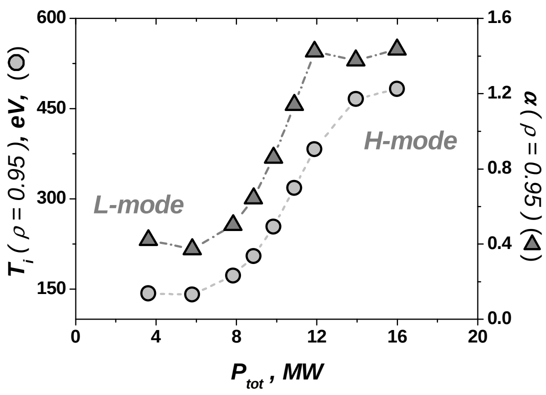

Fig.1 Normalised pressure gradient, α, and ion temperature, at ρ=0.95, vs. the input power.

The capability of the transport code RITM with the transport model outlined above to reproduce both L and H confinement modes, and the transition between them at a critical power, is demonstrated by the results of calculations for JET discharge #53146 characterised by the magnetic field B_T = 2.4T, plasma current I_P = 2.3 MA, elongation and triangularity δ =1.6 and κ = 0.45 []. The deuterium fuelling rate and carbon sputtering coefficient were adjusted to match experimental line averaged density, impurity content and radiation fraction. Figure 1 shows the dependence of the edge normalised pressure gradient, α, and the ion temperature at a characteristic position inside the transport barrier, ρ = 0.95, on the total heating power, P_{tot}, from L-mode conditions at about 3.8 MW and till to the moment when the

H-mode is well established at a power of 16 MW. In a relatively narrow power range of 8-12 MW both characteristics increase very non-linearly by a factor of 3.5. Although these results do not reveal a clear bifurcation between two transport regimes with points where the slop of the curves becomes infinite, there is clear separation between two parameter ranges where both α and T_i are practically independent of power. These power ranges below 6 MW and above 12 MW, and can be attributed to L and H-mode, respectively. Modifications of all parameters and transport characteristics in the transition zone between these two ranges are strongly non-linear interrelated and it is impossible to propose a simple and unique interpretation of the evolution obtained. The next sequence of events seems to us to be the most probable. An increase of the heating power leads to a certain rise of charged particle temperatures at the edge, the plasma collisionality drops and pressure gradient increases. This leads to reduction of the transport driven by Drift Alfven instability, which is the main channel for edge electron particle and heat losses under L-mode conditions. As a result a much steeper density gradient can be formed due to ionisation of recycling neutrals. This allows to keep ITG transport on a low level with increasing ion temperature gradient. Indeed, according to Eq.(8), $\chi^{ITG} \sim \sqrt{\nabla T - \nabla T_{crit}}$ where the critical value of the temperature gradient, ∇T_{crit}, at which the ITG-mode is completely suppressed, increases with the density gradient. Thus, the formation of a strong density gradient due to reduced D^{DA} leads also a decrease of D^{ITG}. In the edge region, where these two major contributors to the transport are damped, the neoclassical transport becomes the leading contribution to χ_I (see fig.2). Formation of this layer with strongly reduced transport, i.e., of the edge transport barrier, leads to the development of a "pedestal" on temperature and pressure profiles.

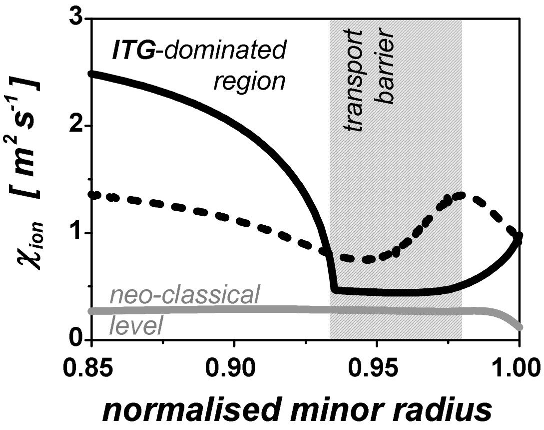

Fig. 2 Radial profiles of ion heat diffusivity computed for the input power 4MW (L-mode, dashed) and 14 MW (H-mode, solid)

The interpretation of the mechanism for the edge barrier maintenance in the H-mode provided above does not rely on the effect of the radial electric field considered normally as the main cause for the turbulence suppression [14]. In order to investigate the relative importance of the density gradient and of the radial electric field in the suppression of ITG at the edge, computations have been performed with these factors included separately and jointly into the consideration. The influence of the radial electric field and the magnetic shear *s* has been taken into account by the formula[]:

$$D_{red}^{ITG} = \frac{D^{ITG}}{1+\left(a_1 \cdot \omega_{ExB}/\gamma_{\max,ITG}\right)^2} \cdot \frac{1}{\max\left(1, \left(s-a_2\right)^2\right)}, \qquad (18)$$

where $\omega_{ExB} = \frac{RB_\theta}{B}\frac{\partial}{\partial r}\left(\frac{E_r}{RB_\theta}\right)$ is **E×B** shearing rate, the coefficient a_1 reflects the fact[14] that the magnitude of the ratio $\omega_{ExB}/\gamma_{\max,ITG}$ needed for the stabilisation of turbulence varies in the range 0.5-2. The term $[\max(1,(s-a_2)^2)]^{-1}$ takes into account that the stabilisation by the magnetic shear takes place only when this exceeds the critical level a_2~1. The radial electric field E_r is calculated from the radial component of the force balance for the main ions, where the toroidal component of ion velocity is put to zero and the poloidal one is given by neoclassical theory [13].

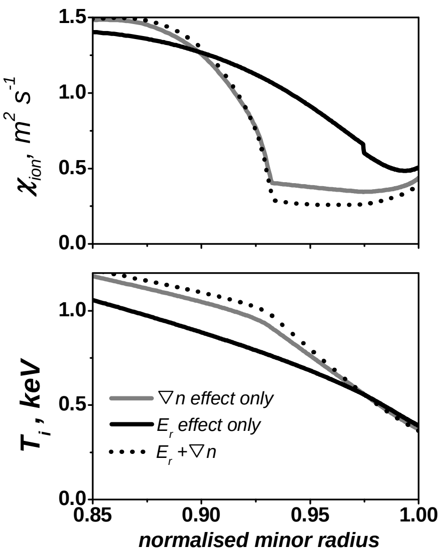

Fig.3 Ion heat conductivity and temperature obtained with different assumptions about the mechanisms for stabilisation of ITG-driven turbulence

Fig.3 shows the profiles of the ion heat conductivity and temperature found for P_{tot}=*10.5 MW*. One can see that the **E×B** rotation shear alone can not lead to formation of a pronounced barrier and the effect of the density gradient is more efficient for this. The obtained result does not mean that the electric field itself does not change significantly from L- to H-mode conditions as it is observed in experiments. This also happens in our computations since E_r is determined by the radial gradients of the plasma parameters, which become much more sharp at the edge in the H-mode.

Presently the code RITM does not allow to model the real time dynamics of the L-H transition, e.g., after an instantaneous increase of P_{tot} above the critical level. The cause is a strongly non-linearity of transport coefficients which does not permit the convergence of calculations for time steps smaller than ~ 10 ms. Therefore the effect of self- generation of plasma poloidal rotation due to Reynold stress and its importance for the dynamics of the edge barrier formation [15] can not be studied in our simulations yet. However, under quasi-stationary conditions considered here, Reynolds stress, probably, does play a considerable role.

4. Comparison to other theories

Recently Guzdar *et al* [16] have developed a theory which explains the transition to H-mode as a result of suppression of drift turbulence by the zonal flow. The suppression of the turbulence induced transport occurs when the dimensionless parameter $\hat{\beta}=\beta(qR/L_n)^2/2$, that determines the growth rate of the zonal flow, exceeds a certain critical value $\hat{\beta}_c$. This criterion can be rewritten in terms of parameter $\Theta = T_e/\sqrt{L_n}$ which has to reach a critical value $\Theta_c = 0.45 B_T(T)^{2/3} Z_{eff}^{1/3}/[R(m)A_i]^{1/6}$ to stabilize the turbulence transport. The results from DIII-D tokamak have shown an excellent agreement between onset of H-mode and condition $\Theta > \Theta_c$, that supports an idea about the crucial role of the density gradient in a suppression of the edge turbulence. Figure 4 shows RITM results where the linear increase of the heating power was done. The quench of ITG-turbulence at the plasma edge starts when Θ reaches the critical level, Θ_c, shown by the horizontal grey line. Such a good agreement of our calculations with Guzdar *et al* [16] is not accidental. The criterion for DA instability suppression proposed by Kerner *et al* [2] can be written in the form:

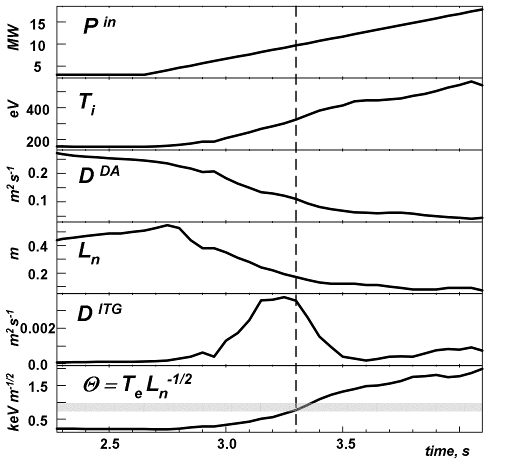

Fig. 4 Time traces for the input power, ion temperature, diffusion coefficient due to DA turbulence, density decay length, diffusion coefficient due to ITG turbulence and parameter Θ at the normalized minor radius of 0.95 during the L-H transition

$$\beta > \frac{L_n^{3/2}}{\lambda_e \sqrt{R}} \left(\frac{8 m_e}{m_i} \right)^{1/2} \approx 0.047 \frac{L_n^{3/2}}{\lambda_e \sqrt{R}}$$

while the Guzdar's condition can be expressed as follows:

$$\beta > \frac{L_n^{3/2}}{\lambda_e \sqrt{R}} \left(\frac{m_e}{m_i q^2} \right)^{1/4} \approx 0.057 \frac{L_n^{3/2}}{\lambda_e \sqrt{R}}$$

where q=4 was assume by estimating the numerical factors. One can see that the difference between two criteria is less than 20%. Therefore, RITM results agree well with the assumption, that the transition occur when Θ approaches its critical value. It is necessary to note here, that not all tokamaks demonstrate the correlation between density gradient and formation of the edge transport barrier. For instance recent results from MAST did not find any indication of a density profile steepening at the edge during the L-H transition [17]. This should be the subject for further investigation.

5. Pedestal characteristics

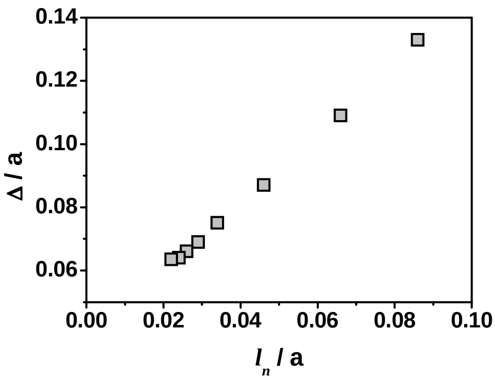

Fig.5 Normalised pedestal width as a function of normalised neutral penetration depth

The characteristics of the edge pedestal, e.g., its width and the temperatures at the pedestal top, $T_{i,e}^{Edge}$, are very important for the overall plasma performance under H-mode conditions [18]. In particular, due to the stiffness of temperature profiles in the plasma core, caused by the nature of turbulence triggered by temperature gradients [5], $T_{i,e}^{Edge}$ control the total plasma thermal energy. The pedestal radial width, Δ, changes in experiments significantly with different global and local plasma parameters [19]. For the profiles computed by RITM the pedestal width is defined as the distance from the separatrix to the position of the maximum ion temperature gradient. The sequence of RITM runs was done to find the relation between Δ and the line-averaged density controlled by the intensity of deuterium fuelling. The decrease of Δ with density is in good correlation with the observations on DIII-D [20] explained by the hypothesis that Δ is controlled by the penetration depth of neutrals, l_n, being inversely proportional to the density. The proportionality between Δ and l_n found by RITM modelling is explicitly demonstrated in Fig.6, showing that pedestal width is controlled by incoming neutrals.

6. Conclusions

The RITM code with the transport model taking into account contributions from different unstable drift modes allows a self-consistent modelling of L and H mode conditions. The edge transport barrier exist due to suppression both of Drift Alfven turbulence with increasing normalised plasma beta and decreasing collisionality and of ITG induced transport suppressed by steep density gradient. Although, *ExB* rotation shear supplementary maintains the edge transport barrier, it is not so important for the suppression of ITG modes as the density gradient. Criteria for the H-mode formation derived in [2] and [16] are close and can be reduced to the requirement that the parameter Θ exceeds a critical level, Θ_c. This requirement is well reproduced in RITM simulations. The width of the barrier is determined by the condition for the suppression of the ITG-mode with the density gradient and scales as the penetration depth of recycling neutrals.

Referencies

[1] Rogers B.N. *et al*, 1998, Phys. Rev. Lett. **81** 4396
[2] Kerner W., *et al*, 1998, Contrib. Plasma Phys. **38** 118
[3] Janeschitz G., *et al*, 1999, J. Nucl. Mater. **266-269** 843
[4] Terry P W 2000 Rev. Mod. Phys. **72**109
[5] Baker D. R. 2001 Phys. Plasmas **8** 4128
[6] Weiland J., 2000, Collective Modes in Inhomogeneous Plasma,
Bristol: Institute of Physics Publishing
[7] Tokar M.Z., 1994, Plasma Phys. and Contr. Fusion **36** 1819
[8] Kadomtsev B.B. and Pogutse O.P., 1971, Nuclear Fusion **11** 67
[9] Tokar M.Z. *et al*, 1999, Plasma Phys. Contr. Fusion **39** L9
[10] Guzdar P.N., 1993, Phys. Fluids **B5** 3712
[11] Horton, W., 1985, Plasma Phys. Contr. Fusion **27** 937
[12] Baker D.R and Rosenbluth M.N., 1998, Phys. Plasmas **5** 2936
[13] Hirshman S P and Sigmar D J 1981 Nucl. Fusion **21** 1079
[14] Burrell K.H. 1997 *Phys. Plasmas* **4** 1499
[15] Diamond P.H., *et al.*, 1994, Phys. Rev. Lett **72** 2565
[16] Guzdar P.N., *et al.*, 2002, Phys. Rev. Lett **89** 265004
[17] Kirk A et al 2004 Plasma Phys. Contr. Fusion **46** 1591
[18] JET team, 2002, Nuclear Fusion **42** 86
[19] Wolf R et al 2003 Plasma Phys. Contr. Fusion **45** 1757
[20] Mahdavi M.A. *et al*, 2002, 29th EPS Conference EPS Conference on Contr. Fusion and Plasma Phys., Montreux, 17-21 June 2002,, ECA Vol. **26B** P-2.098